

UC Merced

UC Merced Electronic Theses and Dissertations

Title

Enigmatic Carbonate Isotope Values in Shark Teeth: Evidence for Environmental and Diet Controls

Permalink

<https://escholarship.org/uc/item/36839713>

Author

Karnes, Molly Elizabeth

Publication Date

2022

Peer reviewed|Thesis/dissertation

UNIVERSITY OF CALIFORNIA, MERCED

**Enigmatic Carbonate Isotope Values in Shark Teeth: Evidence for
Environmental and Diet Controls**

A Thesis submitted in partial satisfaction of the requirements
for the degree of Master of Science

in

Environmental Systems

By

Molly Elizabeth Karnes

Committee in charge:
Professor Sora Kim, Committee Chair
Professor Jessica Blois, Examination Chair
Professor Justin Yeakel

2022

© Copyright

Molly Karnes, 2022

All rights reserved

The Thesis of Molly Karnes is approved, and it is acceptable in quality and form
for publication on microfilm and electronically:

Sora Kim (Committee Chair)

Justin Yeakel

Jessica Blois (Examination Chair)

University of California, Merced

2022

Table of Contents

Symbols	v
List of Tables	vi
List of Figures	vii
Acknowledgments	viii
Abstract	ix
1. Introduction	1
1.1 Tooth organization, structure, and composition.....	1
1.2.1 Oxygen.....	4
1.2.2 Carbon	4
2. Materials and methods	5
2.1 Sample collection.....	5
2.2 Enameloid – carbonate $\delta^{13}\text{C}$ and $\delta^{18}\text{O}$ values	7
2.3 Enameloid – phosphate $\delta^{18}\text{O}$ values	8
2.4 Dentin – organic $\delta^{13}\text{C}$ values	9
2.5 Estimating organic carbon ($\delta^{13}\text{C}$).....	10
3. Results	10
3.1 Modern oxygen isotope compositions	10
3.2 Modern carbon isotope compositions.....	11
3.3 Fossil carbonate analysis	14
4.1 Oxygen isotopes in shark tooth enameloid.....	16
4.1.1 Source water	16
4.1.2 Taxonomic patterns	16
4.1.3 Oxygen offset as a metric for diagenesis	17
4.2 Deconvolving carbon isotopes in shark teeth.....	18
4.2.1 Applications of stable isotope analysis in shark teeth	18
4.2.2 Complications in using $\delta^{13}\text{C}_{\text{CO}_3}$ in sharks.....	19
4.3 Estimated fossil organic carbon values.....	20
5. Conclusions	20
Works Cited	22

Symbols

Abbreviations

SIA – stable isotope analysis

IDE – inner dental epithelium

SLE – shiny-layered enameloid

PBE – parallel-bundled enameloid

TBE – tangled-bundled enameloid

DIC – dissolved inorganic carbon

SIELO – Stable Isotope Ecosystem Lab of the University of California Merced

SIRFER – Stable Isotope Ratio Facility for Environmental Research (University of Utah)

Variables

$\delta^{13}\text{C}_{\text{CO}_3}$ – carbonate carbon isotope value (‰)

$\delta^{13}\text{C}_{\text{org}}$ – organic carbon isotope value (‰)

$\delta^{18}\text{O}_{\text{CO}_3}$ – carbonate oxygen isotope value (‰)

$\delta^{18}\text{O}_{\text{PO}_4}$ – phosphate oxygen isotope value (‰)

$\delta^{13}\text{C}_{\text{org}}^*$ – estimated organic carbon isotope value (‰)

ϵ – fractionation between two isotope values (unitless)

List of Tables

Table 1: The locality, species, and number of modern teeth	6
Table 2: The locality, geologic age, species, and number of fossil teeth	7

List of Figures

Figure 1: Schematic of shark teeth	3
Figure 2: Carbonate oxygen ($\delta^{18}\text{O}_{\text{CO}_3}$) vs. phosphate oxygen ($\delta^{18}\text{O}_{\text{PO}_4}$)	11
Figure 3: Carbonate carbon ($\delta^{13}\text{C}_{\text{CO}_3}$) vs. organic carbon ($\delta^{13}\text{C}_{\text{org}}$)	12
Figure 4: Carbon offset (ϵ) vs. carbonate oxygen ($\delta^{18}\text{O}_{\text{CO}_3}$)	13
Figure 5: Estimated organic carbon ($\delta^{13}\text{C}_{\text{org}^*}$) by geologic age	15

Acknowledgments

I have had many amazing colleagues and friends over the past four years, without whom my research and this thesis would not have been possible.

I would like to start out by thanking my advisor Sora Kim. She believed in me from the very beginning and guided me through developing a project that applied my interest in stable isotope analysis to the intersection of modern and paleo shark ecology. Being her first student at UC Merced, I had the opportunity to see her grow the lab group into a place that is welcoming to everyone and truly feels like family. Her kindness, understanding, and support have helped me overcome many difficulties along the road.

Everyone in our lab group has been supportive and willing to help when needed. Special thanks to Robin Trayler for the numerous hours spent together in the lab teaching me about the many aspects of working in a stable isotope lab: from sample preparation, analysis, standard maintenance on the instruments, data correction. He is also the go-to guy for help with statistics and R code in our lab. My motivation for graduate studies started with an interest in stable isotope analysis, so to have the opportunity to analyze my own samples and hands on experience with the instruments has been truly amazing. I also can't forget our undergraduate students; especially Maya Morris, Pedro Valencia Landa, Alyssa Valdez, and Andrea Diaz Cruz who helped me prepare and weigh samples and just generally made the lab a more fun place to be.

I also would like to thank the funding sources, collaborators, and institutions that supported my research. The Environmental Systems graduate group; the National Science Foundation; NSF grant co-PI's: Michael Griffiths, Kenshu Shimada, Martin Becker, and Robert Eagle; Harry Maisch IV for providing shark teeth to sample; and the Calvert Marine Museum for cataloging specimens.

Moving cross country alone, leaving my friends and support system behind seemed a daunting task at first. I feel truly fortunate to have been welcomed in by the UC Merced community. I especially want to thank close friends: Rachel Chan, Leila Wahab, Ronnie Hall, Melissa Conn, Beth Clifton, Maddie Brown, and Gina Palefsky for always being there for support, whether I needed help with schoolwork, someone to listen, or a shoulder to cry on.

Final thanks go to my partner Corey Ownbey for being patient and always believing in me. For supporting me through the long hours and late nights when deadlines were near and helping with code when I would get too frustrated to think.

Abstract

Enigmatic Carbonate Isotope Values in Shark Teeth: Evidence for Environmental and Diet Controls

By

Molly Karnes

Master of Science in Environmental Systems

University of California, Merced, 2022

Advisor: Sora Kim

Shark teeth are abundant in the fossil record and serve as ancient data buoys, recording physiological information, ecological interactions, and paleo-oceanographic conditions. A tool often used in paleobiological studies to access this recorded information is stable isotope analysis. Fossil shark teeth are well suited for stable isotope analysis because their enameloid is primarily fluorapatite, $\text{Ca}_5(\text{PO}_4)_3\text{F}$, which is resistant to diagenetic alteration due to its high chemical stability. Although often used in paleoecological studies of mammals, carbonate carbon isotope compositions ($\delta^{13}\text{C}_{\text{CO}_3}$) in shark enameloid have remained enigmatic. Here, we investigate multiple stable isotope systems ($\delta^{13}\text{C}_{\text{org}}$, $\delta^{13}\text{C}_{\text{CO}_3}$, $\delta^{18}\text{O}_{\text{CO}_3}$, $\delta^{18}\text{O}_{\text{PO}_4}$) within modern shark teeth to determine relationships between the different systems and build an interpretative framework for future fossil studies. Interestingly, there is no correlation between $\delta^{18}\text{O}_{\text{PO}_4}$ and $\delta^{18}\text{O}_{\text{CO}_3}$ values in modern shark teeth, which contrasts with mammalian studies to date and suggests this metric is not an appropriate test for diagenetic alteration in fossil shark teeth. Organic carbon isotope composition ($\delta^{13}\text{C}_{\text{org}}$) measured from collagen in tooth dentine ranges from -16.0‰ to -10.8‰. Surprisingly, the $\delta^{13}\text{C}_{\text{CO}_3}$ values we measured are much higher, ranging from -6.0‰ to 10.3‰, and there is no direct relationship between $\delta^{13}\text{C}_{\text{org}}$ and $\delta^{13}\text{C}_{\text{CO}_3}$ values in shark teeth. Instead, we found the fractionation (ϵ) between $\delta^{13}\text{C}_{\text{org}}$ and $\delta^{13}\text{C}_{\text{CO}_3}$ values to correspond with $\delta^{18}\text{O}_{\text{CO}_3}$ values but not $\delta^{18}\text{O}_{\text{PO}_4}$ values. It is possible that the source of carbon in shark enameloid is partitioned between dietary carbon and dissolved inorganic carbon (DIC), similar to fish otoliths. We applied the fractionation factor from modern teeth to carbonate isotope composition of fossil shark teeth to predict organic carbon isotope values. The ability to estimate $\delta^{13}\text{C}_{\text{org}}$ values in fossils will provide better insight into carbon cycling and food web dynamics of ancient marine ecosystems.

1. Introduction

Sharks have a rich and abundant fossil record, which documents their persistence through multiple mass extinctions and climate events since their origination in the Devonian. However, paleobiological studies have not explored their evolutionary resilience and ecological plasticity. Previous paleoecological studies of sharks relied primarily on more traditional, descriptive paleontological techniques, but paleobiology is increasingly using quantitative approaches (i.e., biogeochemistry, stable isotope analysis, morphometrics, etc.). Until recently, stable isotope analysis (SIA) of fossil shark teeth was primarily used for paleo-oceanographic reconstructions; however, there is growing interest in using SIA to probe their paleoecology (Kim et al. 2020, Kast et al., accepted, McCormack et al., accepted). These paleoecological studies will benefit from using modern shark teeth as an analog to establish an interpretive framework for future studies relying on stable isotope geochemistry.

The fossil record of sharks is primarily teeth, as their cartilaginous skeletons do not often fossilize. From these teeth, the material best preserved for SIA is the mineralized outer portion of the tooth, known as enameloid, which is highly resistant to chemical alteration (Vennemann et al. 2001, Enax et al. 2012). Modern shark ecology is beginning to utilize SIA of teeth, however most neontological studies focus on the organic, dentine portion of the tooth (Polo-Silva et al. 2012, Zeichner et al. 2017, Shipley et al. 2021). Given the availability of modern shark teeth, we can investigate a range of stable isotope systems to bridge our knowledge of modern and paleo shark ecology. However, carbonate carbon isotope values ($\delta^{13}\text{C}_{\text{CO}_3}$) remain enigmatic due to their unusually high values. This phenomenon has been noted for fossil (Ounis et al. 2008, Van Baal et al. 2013, Kocsis et al. 2014) and modern sharks (Vennemann et al. 2001). Preliminary data lack the linear relationship between inorganic and organic carbon isotope values that is seen in mammals. In addition to the carbon isotope relationship, the differentiation between carbonate and phosphate oxygen isotope values ($\delta^{18}\text{O}_{\text{CO}_3}$ and $\delta^{18}\text{O}_{\text{PO}_4}$, respectively) warrants further investigation given previous studies (Venneman et al. 2001).

1.1 Tooth organization, structure, and composition

Sharks have a polyphyodont dentition and a unique process of tooth replacement using a “conveyor belt” style (Figure 1A/B, Berkovitz and Shellis 2017a). The teeth are organized into multiple rows oriented along the jaw (Figure 1A). A series of teeth is a set of teeth perpendicular to the jaw that are at different stages of development (Figure 1B). Teeth at the buccal edge of the jaw are the oldest row of teeth and are referred to as “functional teeth” (Figure 1B). Sampling along a tooth series allows us to study temporal changes that occur, such as ontogenetic shifts and seasonal migration. Functional teeth are replaced every few weeks, depending on the species

(Berkovitz and Shellis 2017a). This style of lifelong tooth replacement is the reason why shark teeth are incredibly abundant in the fossil record.

Most shark teeth are composed of a central region of dentine covered by a layer of enameloid approximately 0.2-0.9mm that is thinner near the tooth root and thickens towards the tip (Figure 1C, Vennemann et al., 2001). This enameloid layer performs the same function as mammalian enamel but differs in the origin of formation. Enamel is formed by the inner dental epithelium (IDE) and enameloid forms in between the IDE and the ectomesenchymal cells of the dental papilla (Berkovitz and Shellis 2017b). Structurally, the enameloid consists of three main layers: shiny-layered enameloid (SLE), parallel-bundled enameloid (PBE), and tangled-bundled enameloid (TBE) (Enax et al. 2014). Mineralogically, enameloid is a fluoride-rich biogenic apatite primarily composed of fluorapatite ($\text{Ca}_5(\text{PO}_4)_3\text{F}$) with occasional substitutions of hydroxide for fluoride ($\text{Ca}_5(\text{PO}_4)_3\text{OH}$, hydroxyapatite) and carbonate for phosphate ($\text{Ca}_5(\text{PO}_4, \text{CO}_3)_3\text{F}$, carbonated apatite) (Moeller et al. 1975, Miake et al. 1991). It also contains <5% organic matrix (Sire et al. 2007). The high fluoride concentration and low organic content make it more resistant to diagenetic alteration than dentin or bone. In contrast, dentine has a much higher organic content of 15-20% (Enax et al. 2012) making it more susceptible to diagenetic alteration than enameloid. (Hättig et al. 2019).

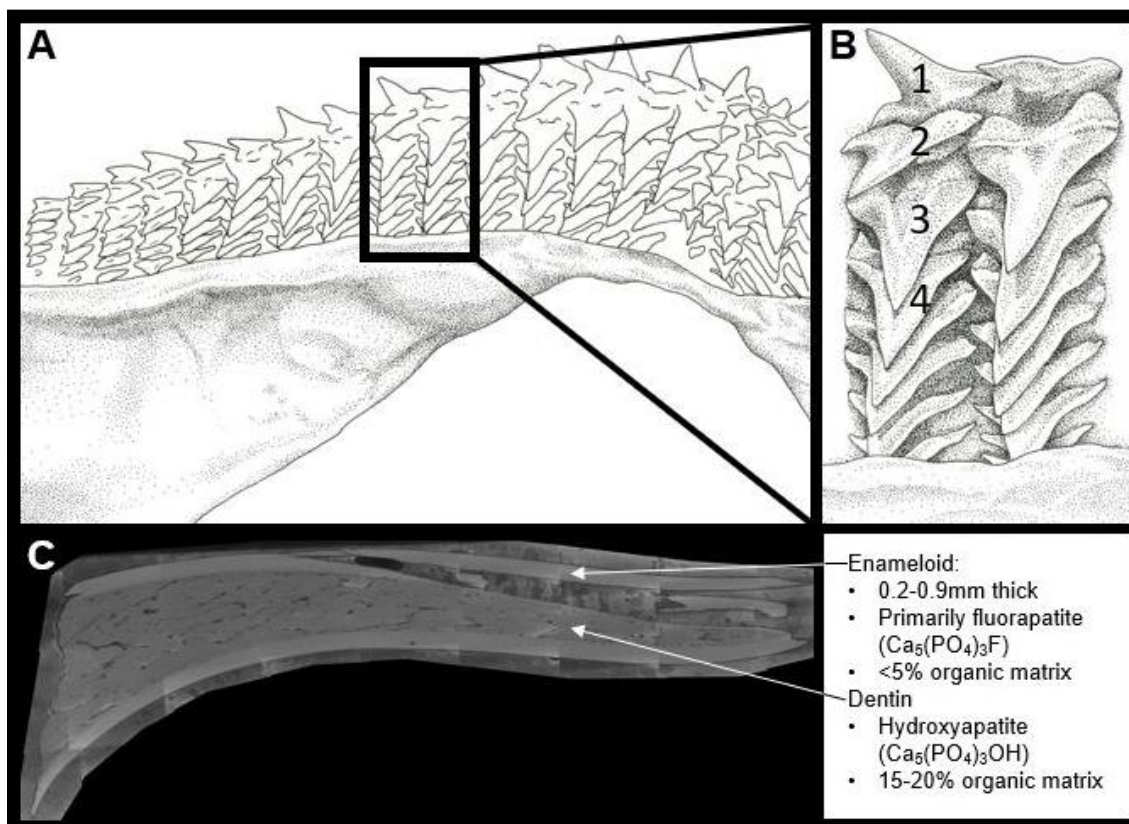


Figure 1: A: Sketch of a shark jaw and teeth (*Sphyrna mokarran*, great hammerhead shark) showing the arrangement of teeth within a jaw. Rows are parallel and series are perpendicular to the jaw. B: A closer look showing two series of teeth, teeth are numbered from the buccal edge of the jaw with 1 being the oldest tooth (functional tooth). Sketches done by Sarah Baird. C: SEM cross section image of a modern shark tooth (*Carcharias taurus*, sand tiger shark). Image generated by James Schiffbauer at the University of Missouri X-ray microanalysis lab (MizzouμX). Arrows show the regions of enameloid and dentine. The tooth is embedded in resin, as the tip of the tooth is fractured.

1.2 Stable Isotope Systems

Stable isotope analysis is a commonly used tool in both modern and paleo-ecological studies to answer questions about diet and food web structure, including changes through ontogeny and migration. These types of studies typically analyze soft tissue for organic isotope composition (i.e., carbon and nitrogen); however, teeth also provide a substrate for investigating these ecological and environmental questions. Dental collagen extracted from dentin can also be analyzed for organic carbon and nitrogen ($\delta^{13}\text{C}_{\text{org}}$ and $\delta^{15}\text{N}_{\text{org}}$) which are recorders of trophic interactions and movement (Zeichner et al. 2017, Shipley

et al. 2021). In contrast, enameloid is often analyzed for oxygen isotope composition of the mineral portion, which records chemical signals from the environment at the time of formation (Vennemann et al., 2001). Paleontological studies use enameloid oxygen isotope values (i.e., $\delta^{18}\text{O}_{\text{CO}_3}$ and $\delta^{18}\text{O}_{\text{PO}_4}$) as proxies for salinity (Kim et al. 2014, Sisma-Ventura et al. 2019) and temperature (Lecuyer et al. 2003, Zacke et al. 2009, Fischer et al. 2012) in paleoceanographic studies. To date, carbon isotope values in carbonate ($\delta^{13}\text{C}_{\text{CO}_3}$) are thought to incorporate aspects of diet (Cerling and Harris 1999, Passey et al. 2005) but the existing interpretation is based on work with mammals. This framework does not seem valid for sharks given the isotope relationships we report in this study.

1.2.1 Oxygen

Oxygen isotope compositions of teeth vary based on the $\delta^{18}\text{O}$ value of body water and the temperature at time of formation (Kolodny et al. 1983, Kohn and Cerling 2002, Pucéat et al. 2010). In endotherms, this temperature dependency is regulated by body temperature; however, in ectotherms (most sharks), body temperature reflects environmental temperature. Because of this relationship to environmental temperature, the $\delta^{18}\text{O}$ value of shark teeth is often used as a paleothermometer (Vennemann and Hegner 1998, Fischer et al. 2012, Tütken et al. 2020). In biogenic phosphates like enameloid, $\delta^{18}\text{O}$ values can be measured in both phosphate and carbonate. It is assumed that as the tooth forms, the phosphate and carbonate oxygen isotope systems are in equilibrium with the same pool of body water and therefore should have a constant offset (Kohn and Cerling 2002). The expected carbonate-phosphate oxygen isotope offset is $\sim 9\text{‰}$ and this value is often used as a check for diagenetic alteration in fossil specimens (Bryant et al. 1996, Iacumin et al. 1996, Kohn and Cerling 2002, Zazzo et al. 2004, Martin et al. 2008). However, this expected offset is based on mammals and previous studies report a large and inconsistent offset in sharks ($6.0\text{--}11.8\text{‰}$; Vennemann et al. 2001). This result suggests that earlier assumptions about the relationship between carbonate and phosphate oxygen isotope composition may not hold true for sharks.

1.2.2 Carbon

Organic carbon isotope values ($\delta^{13}\text{C}_{\text{org}}$) are incorporated into consumer tissues via diet, which traces energy flow through a food web with an average fractionation of $\sim 1\text{‰}$ between trophic levels (DeNiro and Epstein 1978). Primary producers set the isotopic baseline of an ecosystem. In terrestrial ecosystems,

the main difference in carbon isotope fractionation is in C3 vs. C4 photosynthetic pathways (Farquhar et al. 1989). In marine systems, the range represents the availability of fresh CO₂ sources for photosynthesis and the organisms' ability to fully express isotopic discrimination that can differentiate littoral and pelagic dietary sources (Casey and Post 2011).

Inorganic carbon in bioapatite is related to organic dietary carbon through respiration. Respired metabolic CO₂ in blood is in isotopic equilibrium with enamel at time of formation (Passey et al. 2005). In mammals, enamel $\delta^{13}\text{C}_{\text{CO}_3}$ values are closely related to $\delta^{13}\text{C}_{\text{org}}$ values (Codron et al. 2018) and suggests that both $\delta^{13}\text{C}_{\text{org}}$ and $\delta^{13}\text{C}_{\text{CO}_3}$ values reflect diet. In some marine organisms, $\delta^{13}\text{C}_{\text{CO}_3}$ values in biomineralized substrate record a more complicated signal that confounds diet and environmental inputs. For example, $\delta^{13}\text{C}_{\text{CO}_3}$ values in otoliths (fish ear stones) are a combined signal from respiration of ingested prey and dissolved inorganic carbon (DIC) in water, with the relative proportions controlled by metabolism (Chung et al. 2019). Given that the enameloid of shark teeth is maturing in contact with seawater, we hypothesize similar processes may affect both carbonate carbon and oxygen isotope compositions.

To investigate the isotopic relationships and create a modern interpretive framework for shark teeth, we compiled an array of modern shark teeth and analyzed the stable isotope composition of the following systems: phosphate oxygen ($\delta^{18}\text{O}_{\text{PO}_4}$), carbonate oxygen ($\delta^{18}\text{O}_{\text{CO}_3}$), carbonate carbon ($\delta^{13}\text{C}_{\text{CO}_3}$), and organic carbon ($\delta^{13}\text{C}_{\text{org}}$). We find limited relationships between $\delta^{18}\text{O}_{\text{PO}_4}$ and $\delta^{18}\text{O}_{\text{CO}_3}$ values as well as $\delta^{13}\text{C}_{\text{CO}_3}$ and $\delta^{13}\text{C}_{\text{org}}$ values, but propose an explanation based on the correlation of $\delta^{18}\text{O}_{\text{CO}_3}$ values to carbon enrichment values. Then, we use this relationship to estimate the organic carbon isotope values from fossil shark teeth.

2. Materials and methods

2.1 Sample collection

Powdered dentin and enameloid samples were collected from 153 modern shark teeth, including wild and aquarium kept individuals, some of which were part of a previously published captive feeding study (Kim et al. 2012a, 2012b). The *Sphyrna zygaena* (smooth hammerhead shark) teeth were extracted from a formalin-preserved specimen from the University of Utah collections. This dataset includes individuals from eight families (Carcharhinidae, Lamnidae, Megachasmidae, Odontaspidae, Somniosidae, Sphyrnidae, Squalidae, and Triakidae; Table 1).

Powdered enameloid samples were also collected from 59 fossil shark teeth that range from Cretaceous to Pliocene in age and include six families (Anacoracidae, Carcharhinidae, Lamnidae, Mitsukurinidae, Odontaspidae, and Odontidae; two individuals from an uncertain family (*Parotodus benedini*); Table 2). In addition to data generated in this study, we also included previously published data from Eocene Arctic and tiger sharks (family: Odontaspidae) (Kim et al. 2014). Localities, age, species, and number of all fossils are included in Table 1. All modern and fossil specimens are catalogued at the Calvert Marine Museum and specimen identification numbers are included in the supplemental data table.

Modern Teeth Localities and Species		
Location	Species	n
Delaware Bay	<i>Carcharias taurus</i>	39
Santa Cruz, California (captive)	<i>Triakis semifasciata</i>	7
Japan	<i>Carcharhinus brevipinna</i>	1
	<i>Centrophorus acus</i>	6
	<i>Centroscymnus owstoni</i>	1
	<i>Mustelus manazo</i>	1
	<i>Sphyrna zygaena</i>	5
New York Aquarium	<i>Carcharhinus plumbeus</i>	15
	<i>Carcharias taurus</i>	15
Florida	<i>Carcharhinus limbatus</i>	5
South Africa	<i>Carcharhinus leucas</i>	19
	<i>Carcharhinus obscurus</i>	5
	<i>Carcharodon carcharias</i>	6
	<i>Galeocerdo cuvier</i>	9
	<i>Sphyrna mokarran</i>	4
Unknown	<i>Lamna ditropis</i>	3
	<i>Megachasma plegios</i>	1
	<i>Odontaspis ferox</i>	3
Unknown	<i>Sphyrna zygaena</i>	8

Table 1: The locality, species, and number of all modern teeth included in this study.

Fossil Teeth Localities and Species					
Location	Formation	Period	Age	Species	n
Bakersfield/ Santa Cruz	Temblor	Miocene	Langhian	<i>Carcharhinus sp.</i>	2
				<i>Carcharodon carcharias</i>	1
				<i>Carcharodon hastalis</i>	1
				<i>Isurus planus</i>	1
				<i>Otodus megalodon</i>	3
				<i>Physogaleus sp.</i>	1
Aurora, NC	Pungo River	Miocene	Burdigalian- Langhian	<i>Carcharias sp.</i>	2
				<i>Carcharias taurus</i>	1
				<i>Carcharodon hastalis</i>	1
				<i>Otodus chubutensis</i>	1
	Yorktown	Pliocene	Zanclean- Piazencian	<i>Carcharhinus sp.</i>	1
				<i>Carcharias taurus</i>	1
				<i>Otodus megalodon</i>	8
				<i>Carcharodon carcharias</i>	3
				<i>Carcharodon hastalis</i>	1
				<i>Isurus oxyrinchus</i>	3
<i>Parotodus benedini</i>	1				
Inshore Ledge, NC		Miocene		<i>Otodus chubutensis</i>	1
Kuzubukuro/ Chochi City (JPN)	Iwadono	Miocene	Burdigalian- Langhian	<i>Otodus megalodon</i>	1
				<i>Parotodus benedini</i>	1
	Naarai	Pliocene	Zanclean	<i>Carcharodon carcharias</i>	1
				<i>Otodus megalodon</i>	7
N. Banks Island (Canada)	Eureka Sound	Eocene		<i>Striatolamia macrota</i>	20
Alabama		Eocene		<i>Striatolamia macrota</i>	1
Alabama		Cretaceous	Santonian	<i>Scapanorhynchus texanus</i>	1
Arkansas		Cretaceous		<i>Carcharias holmdelensis</i>	1
Florida		Miocene		<i>Otodus megalodon</i>	1
New Jersey		Eocene		<i>Striatolamia macrota</i>	1
South Carolina		Pliocene		<i>Carcharodon hastalis</i>	2
France		Cretaceous	Campanian	<i>Scapanorhynchus sp.</i>	1
				<i>Squalicorax kaupi</i>	1
Kazakhstan		Eocene		<i>Otodus sokolovi</i>	1
Morocco		Eocene		<i>Striatolamia macrota</i>	1

Table 2: The locality, geologic age, species, and number of all fossil teeth included in this study.

2.2 Enameloid – carbonate $\delta^{13}\text{C}$ and $\delta^{18}\text{O}$ values

For the analysis of enameloid, 4-5mg of sample were collected from all shark teeth using a Dremel on low speed with a 300-micron diamond tipped bit. These samples were then treated with 2.5% NaOCl overnight to remove organic contaminants, rinsed five times with deionized water and dried overnight in an

oven at $\sim 50^{\circ}\text{C}$. Modern samples were then split into two portions for carbonate and phosphate preparation.

Fossil samples need an additional treatment of acetic acid to remove potential secondary carbonates before subsequent chemistry was performed (Trueman et al. 2004). Once samples had been rinsed of NaOCl, 0.5 mL 1M acetic acid buffered to pH ~ 5 with 0.91M calcium acetate was added. Samples were allowed to react in the refrigerator for 24 hours. After reaction, samples were rinsed five times with deionized water and dried in an oven at $\sim 50^{\circ}\text{C}$.

For carbonate analysis, samples were weighed to ~ 0.5 mg into glass exetainers (3.7 mL round bottom vial, Labco). The headspace of the vials was flushed with He gas. Samples were heated to 27°C and 1.0 mL of 104% phosphoric acid was added and allowed to digest fully. This reaction produces CO_2 , which was measured for $\delta^{13}\text{C}$ and $\delta^{18}\text{O}$ values using a GasBench coupled to a Delta V Plus continuous flow isotope ratio mass spectrometer with a Conflo IV at the Stable Isotope Ecosystem Lab of the University of California Merced (SIELO). We determined $\delta^{13}\text{C}$ and $\delta^{18}\text{O}$ relative to Vienna Pee Dee Belemnites (VPDB). Data were corrected for linearity and drift using a suite of calibrated reference materials (Carrara Marble [n = 28], NBS 18 [n = 31], USGS 44 [n = 30]). Long-term standard deviation for the instrument is $\pm 0.2\text{‰}$ for both $\delta^{13}\text{C}$ and $\delta^{18}\text{O}$ values.

The *S. zygaena* samples from the University of Utah collections were weighed to ~ 0.25 mg into glass exetainers that were then flushed with He gas. Samples underwent acid digestion via phosphoric acid. The resulting CO_2 was measured for $\delta^{13}\text{C}$ and $\delta^{18}\text{O}$ values on a Thermo Finnigan Gas Bench II connected to a Thermo Finnigan MAT 253 via Conflo IV at the Stable Isotope Ratio Facility for Environmental Research (SIRFER) at the University of Utah. All data were corrected using a suite of calibrated reference materials (LSVEC [n = 4] as well as Carrara [n = 4] and Marble [n = 3], both internal lab standards are calibrated against international reference materials). Long-term standard deviation for the instrument is $\pm 0.2\text{‰}$ for both $\delta^{13}\text{C}$ and $\delta^{18}\text{O}$ values.

2.3 Enameloid – phosphate $\delta^{18}\text{O}$ values

For phosphate oxygen isotope analysis, the subsample of enameloid powder as described in 2.2 was used to precipitate silver phosphate using the “rapid” precipitation method from Mine et al. (2017). First, 1.5 mg of sample were dissolved in 50 μL 2M HNO_3 overnight. The next day, CaF_2 was precipitated using 30 μL 2.9M HF and 50 μL 2M NaOH and the supernatant was transferred

to a new microcentrifuge tube. The CaF_2 pellet was rinsed with 50 μL 0.1M NaF and this supernatant was also transferred to the new tube. Silver phosphate was precipitated from the supernatant by adding 180 μL of a silver ammine solution (0.37M AgNO_3 , 1.09M NH_4OH) and the pH was adjusted to 6-7 using dilute HNO_3 . This pH window is important so that all phosphate is precipitated from solution, which prevents isotopic fractionation of oxygen. Silver phosphate crystals were rinsed five times with deionized water and dried overnight at 50°C. All phosphate samples were weighed in triplicate to 0.15 – 0.20 mg in silver capsules and measured for $\delta^{18}\text{O}$ values using a TC/EA coupled to a Delta V Plus continuous flow isotope ratio mass spectrometer with a Conflo IV at the SIELO. We determined $\delta^{18}\text{O}$ relative to Vienna Standard Mean Ocean Water (VSMOW). All data were corrected for linearity and drift using a suite of calibrated reference materials (USGS 80 [n = 95], USGS 81a [n = 91], IAEA 601 [n = 52]). Long-term standard deviation for the instrument is $\pm 0.4\text{‰}$ for $\delta^{18}\text{O}$.

2.4 Dentin – organic $\delta^{13}\text{C}$ values

To determine the stable isotope composition of organic carbon ($\delta^{13}\text{C}_{\text{org}}$), collagen was isolated from tooth dentine. Powdered dentine samples were collected from all modern shark teeth using a Dremel on low speed with a 300-micron diamond tipped bit. These samples were then demineralized using chilled 0.1M HCl following Trayler et. al (in prep). After demineralization, samples were rinsed five times with deionized water and freeze dried overnight. Samples were weighed to 0.4-0.5 mg in 3x5 mm tin capsules. Collagen samples were measured for $\delta^{13}\text{C}$ values using a Costech 4010 Elemental Analyzer coupled to a Delta V Plus continuous flow isotope ratio mass spectrometer with a Conflo IV at the SIELO. All data were corrected for linearity and drift using a suite of calibrated reference materials (USGS 40 [n = 36], USGS 41a [n = 23], costech acetanilide [n = 35]). Long-term standard deviation for the instrument is $\pm 0.1\text{‰}$ for $\delta^{13}\text{C}$ values.

For the *S. zygaena* specimens from the University of Utah collections, dentin was demineralized in 0.6N HCl at 4°C. The supernatant was decanted and replaced daily until complete (supernatant free of $\text{Ca}_3(\text{PO}_4)_2$, no visible density gradient, and sample “spongy” when probed). The sample was then rinsed to neutrality and soaked in 5% KOH. The KOH was poured off and replaced daily for removal of organic contaminants. After acid and base extraction, the sample was rinsed to neutrality again and gelatinized in 5 ml of water (pH 3) for 24 hours at 90°C. Water-soluble and insoluble phases were then separated by filtration

with a 0.45 micron, Luer-Lok syringe filter and the water-soluble phase was lyophilized and weighed to obtain a final collagen yield. Collagen samples were measured for $\delta^{13}\text{C}$ values by flash combustion on a continuous-flow isotope ratio mass spectrometer coupled to elemental analyzer at SIRFER. All data were corrected for linearity and drift using a suite of calibrated reference materials (UU-CN-1 [n = 3], UU-CN-2 [n = 3], both internal lab standards are glutamic acids calibrated against USGS 40 and USGS 41). Long-term standard deviation for the instrument is $\pm 0.2\text{‰}$ for $\delta^{13}\text{C}$ values.

2.5 Estimating organic carbon ($\delta^{13}\text{C}$)

We compared the offset between the two $\delta^{13}\text{C}$ values ($\delta^{13}\text{C}_{\text{CO}_3}$ and $\delta^{13}\text{C}_{\text{org}}$), based on the fractionation (ϵ), which is sometimes referred to as the “per mil fractionation,” and defined as:

$$\alpha = \left(\frac{(1000 + \delta^{13}\text{C}_{\text{CO}_3})}{(1000 + \delta^{13}\text{C}_{\text{org}})} \right)$$

$$\epsilon = 1000 * \ln(\alpha).$$

This calculation of fractionation was chosen over the simpler $\Delta_{\text{A-B}} = \delta_{\text{A}} - \delta_{\text{B}}$ because $\Delta_{\text{A-B}}$ is only a good approximation of fractionation when values are $< 10\text{‰}$. Additionally, we used only functional teeth (position 1, Figure 1) for the regression as the carbon offset varies between teeth in different positions, possibly due to changing CO_3 concentration during enameloid maturation.

3. Results

3.1 Modern oxygen isotope compositions

We used a single tooth to generate carbonate and phosphate $\delta^{18}\text{O}$ values from 117 modern specimens. We generated only $\delta^{18}\text{O}_{\text{CO}_3}$ values for an additional 36 modern specimens. For our dataset, the $\delta^{18}\text{O}_{\text{CO}_3}$ range from 23.3‰ to 30.9‰, with an average of 27.0‰ (n = 153). The range for $\delta^{18}\text{O}_{\text{PO}_4}$ values was narrower than that for $\delta^{18}\text{O}_{\text{CO}_3}$ values, ranging from 20.1‰ to 24.8‰, with an average of 22.8‰ (n = 117). The offset between $\delta^{18}\text{O}_{\text{CO}_3}$ and $\delta^{18}\text{O}_{\text{PO}_4}$ values ranges from 0.3 to 7.5‰ with an average of 4.3‰. Pearson’s correlation shows a significant but low positive correlation between $\delta^{18}\text{O}$ values from carbonate and phosphate across all specimens ($r = 0.44$, $p = 1.09 \times 10^{-6}$). A comparison at the family level demonstrated a stronger positive correlation for Carcharhinidae (n=49; $r = 0.70$, $p = 7.49 \times 10^{-9}$). However, other families had weaker correlations than the entire

sample set. For example, Odontaspidae had extensive variation, which spanned nearly the entire range of values ($\delta^{18}\text{O}_{\text{CO}_3}$ ranged 6.1‰ and $\delta^{18}\text{O}_{\text{PO}_4}$ ranged 4.0‰), but there was very low, but significant correlation ($r = 0.29$, $p = 0.03$). Another notable family is Lamnidae, where all individuals had elevated $\delta^{18}\text{O}$ values (i.e., plotted together in the upper right quadrant; Figure 2).

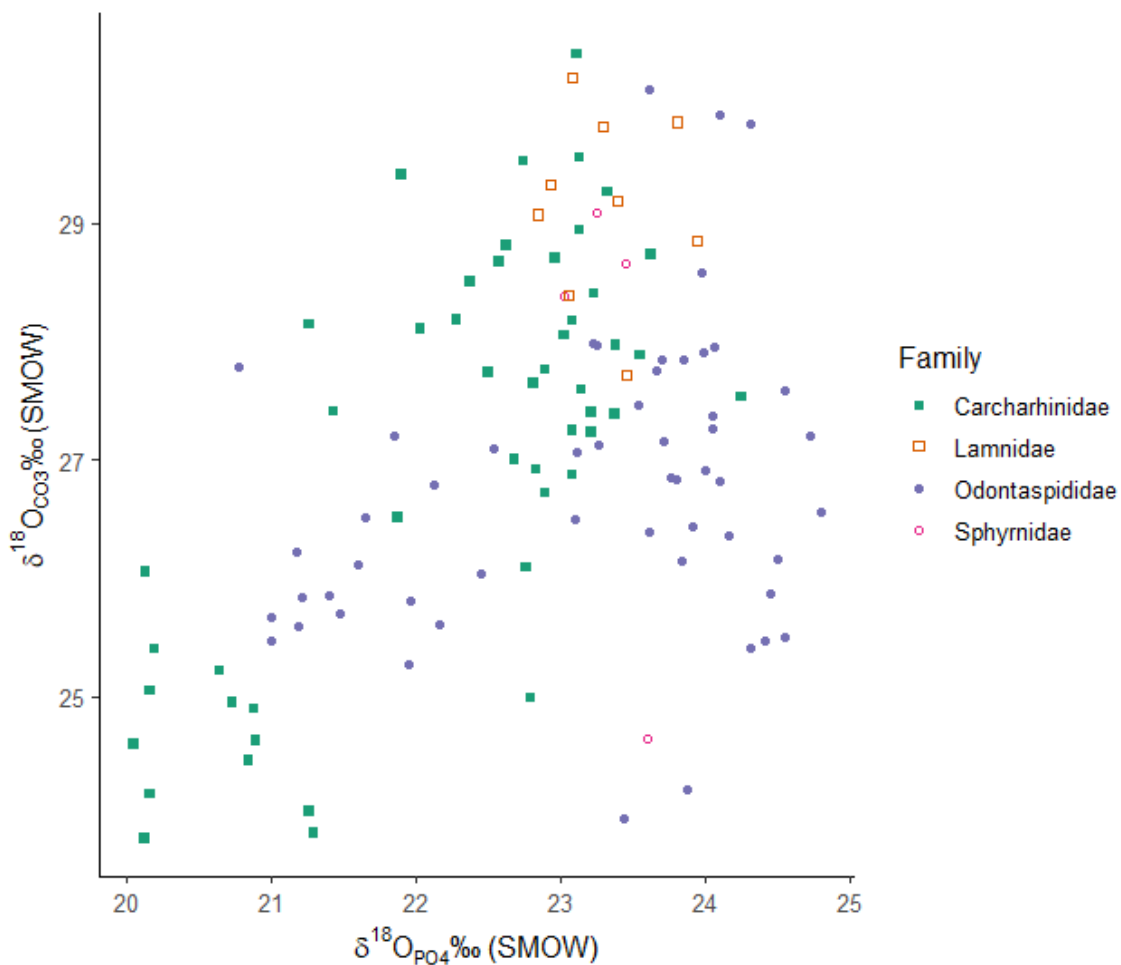


Figure 2: Phosphate oxygen ($\delta^{18}\text{O}_{\text{PO}_4}$) vs. carbonate oxygen ($\delta^{18}\text{O}_{\text{CO}_3}$) isotope composition. Colors represent different families. There is weak correlation between these variables (see text).

3.2 Modern carbon isotope compositions

We generated $\delta^{13}\text{C}$ values of collagen ($\delta^{13}\text{C}_{\text{org}}$) and carbonate ($\delta^{13}\text{C}_{\text{CO}_3}$) from 151 modern specimens. The wild specimens have $\delta^{13}\text{C}_{\text{org}}$ values that range from -16.7‰ to -11.1‰, with an average of -13.8‰ ($n = 146$). There are five

individuals with low $\delta^{13}\text{C}_{\text{org}}$ values; four of these individuals were part of a captive controlled feeding experiment and were intentionally fed a ^{13}C depleted diet. The mean C:N of modern samples was 3.0 ± 0.7 and there was no distinction by family. The $\delta^{13}\text{C}_{\text{CO}_3}$ values have a wider range, ranging from -5.4‰ to 10.3‰ , with an average of 2.3‰ ($n = 151$). Pearson's correlation shows there is no correlation between $\delta^{13}\text{C}_{\text{org}}$ and $\delta^{13}\text{C}_{\text{CO}_3}$ ($r = 0.17$, $p = 0.04$).

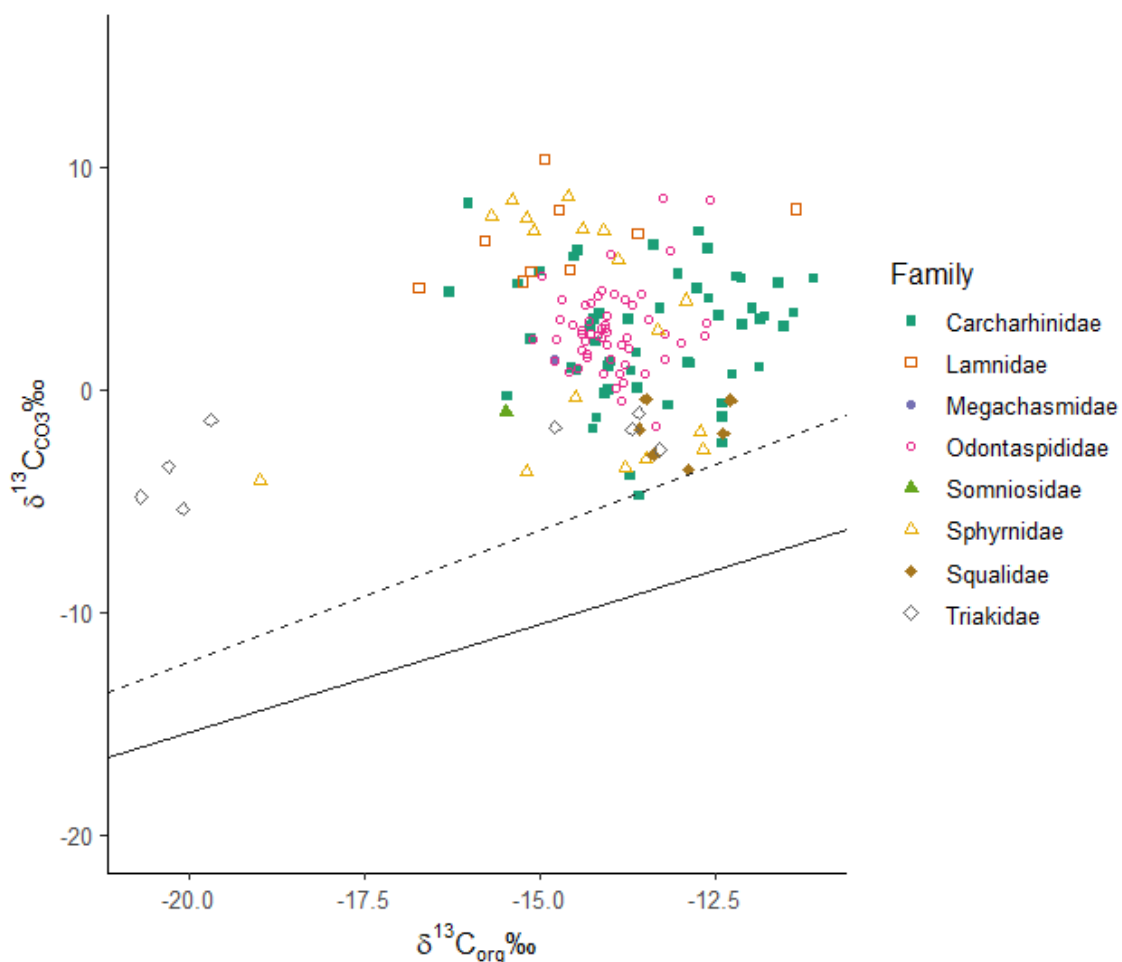


Figure 3: Organic carbon ($\delta^{13}\text{C}_{\text{org}}$) vs. carbonate carbon ($\delta^{13}\text{C}_{\text{CO}_3}$) isotope values with the same coloration by family as Figure 2. There is no correlation between these variables in contrast to results from mammals, which is shown by the lines. The dashed line is the best fit for herbivore mammals and solid line is the best fit for carnivore mammals ($r^2 > 0.89$ and p -values < 0.0001 ; Codron et al. 2018).

The ϵ values range 16.4‰ from 8.9 to 25.3‰, with an average of 16.4‰. Further, this offset has a significant correlation with $\delta^{18}\text{O}_{\text{CO}_3}$ values ($r^2 = 0.62$, $p = <2.2 \times 10^{-16}$), but only marginal coherence with $\delta^{18}\text{O}_{\text{PO}_4}$ values ($r^2 = 0.03$, $p = 0.05$). The relationship between ϵ and $\delta^{18}\text{O}_{\text{CO}_3}$ is described by a linear model, $\epsilon = ((1.54 \pm 0.1) * \delta^{18}\text{O}_{\text{CO}_3}) + (22.64 \pm 0.5)$. We did not find distinctions in relationship by family.

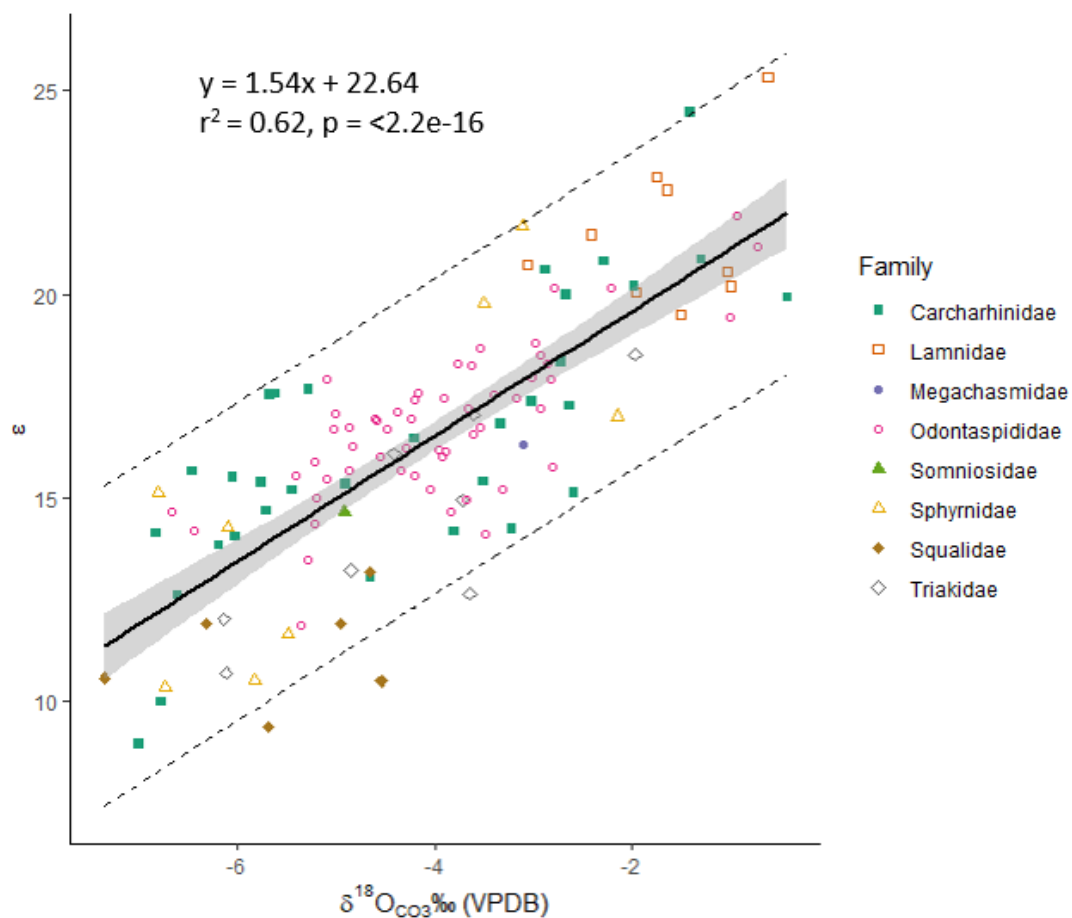


Figure 4: The carbon fractionation ($\epsilon = 1000 \cdot \ln(\alpha)$) compared to carbonate oxygen isotope composition ($\delta^{18}\text{O}_{\text{CO}_3}$). A linear regression of the data is in black ($y = 1.54x + 22.64$, $r^2 = 0.62$, $p = <2.2 \times 10^{-16}$), with the 95% confidence interval shaded. The dashed lines represent the 95% prediction interval. Points are colored by family.

3.3 Fossil carbonate analysis

We generated carbonate data ($\delta^{13}\text{C}_{\text{CO}_3}$ and $\delta^{18}\text{O}_{\text{CO}_3}$ values) from 54 fossil specimens. The fossils include four geologic periods: Cretaceous (145 Ma – 66 Ma, $n = 4$), Eocene (56 Ma – 33.9 Ma, $n = 24$), Miocene (23.03 Ma – 5.333 Ma, $n = 18$), and Pliocene (5.333 Ma – 2.58 Ma, $n = 28$) (localities are listed in Table 1). For our dataset, the $\delta^{13}\text{C}_{\text{CO}_3}$ values range from -3.1‰ to 9.6‰ , with an average of 4.5‰ ($n = 54$). The $\delta^{18}\text{O}_{\text{CO}_3}$ values range from 19.5‰ to 28.3‰ , with an average of 26.1‰ ($n = 54$).

3.4 Estimating fossil organic carbon values

Given the strong relationship between ϵ and $\delta^{18}\text{O}_{\text{CO}_3}$ values in modern teeth, we apply the linear model from Figure 4 to fossil teeth and estimate organic $\delta^{13}\text{C}$ values. We refer to estimated organic carbon isotope composition as $\delta^{13}\text{C}_{\text{org}^*}$ values. The mean and standard deviation of each time bin are as follows: Cretaceous = $-8.6 \pm 1.6\text{‰}$, Eocene = $-3.3 \pm 5.9\text{‰}$, Miocene = $-10.5 \pm 1.3\text{‰}$; and Pliocene = $-11.7 \pm 2.4\text{‰}$ (Figure 5). In general, the $\delta^{13}\text{C}_{\text{org}^*}$ values from fossil shark teeth had a larger variation and were more depleted in ^{13}C than modern shark teeth.

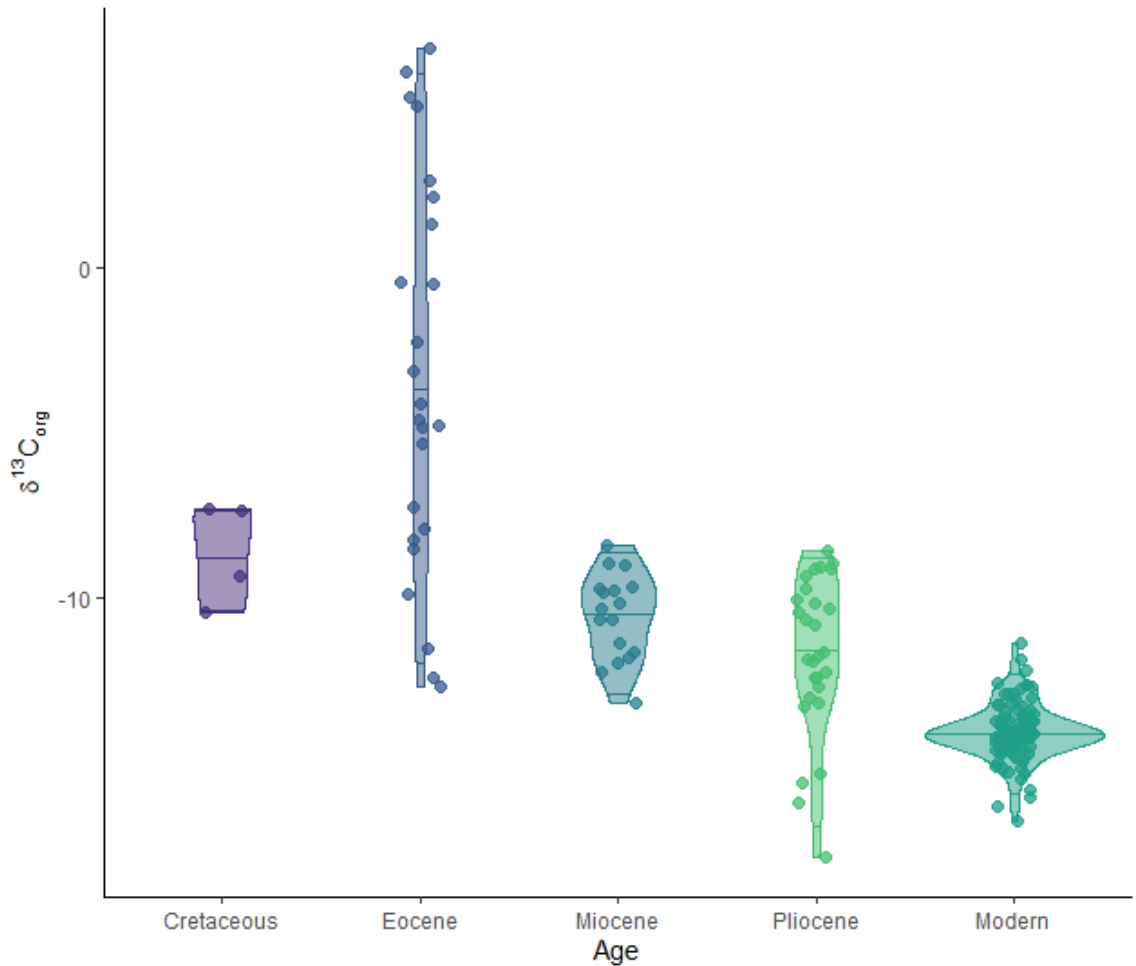


Figure 5: Organic carbon isotope values by geologic age of teeth. Modern values are measured from analysis of dental collagen and fossil values are estimated using the regression equation from Figure 4 ($\delta^{13}\text{C}_{\text{org}}^*$).

4. Discussion

We generated a suite of stable isotope values from modern shark teeth to investigate the interrelationships between organic and mineral isotope systems as well determine paleoecological applications. We discuss patterns between oxygen isotopes in carbonate and phosphate as well as carbon in organic and carbonate substrates, while also comparing our patterns to those from mammals, a well-studied system. Further, we apply a model based on modern shark teeth to carbonate isotope results from fossil shark teeth to explore the possible implications for paleoecological studies.

4.1 Oxygen isotopes in shark tooth enameloid

4.1.1 Source water

We expected $\delta^{18}\text{O}_{\text{CO}_3}$ and $\delta^{18}\text{O}_{\text{PO}_4}$ in enameloid to have a strong linear relationship. This is because both oxygen isotope components are thought to form synchronously in equilibrium with the same body source water during enameloid mineralization. However, we found only a weak correlation between $\delta^{18}\text{O}_{\text{CO}_3}$ and $\delta^{18}\text{O}_{\text{PO}_4}$ values in shark tooth enameloid (Figure 2), which suggests these components are recording different signals. Experiments with synthetic apatite minerals show that $\delta^{18}\text{O}$ values are controlled by a kinetic fractionation process that involves the $\delta^{18}\text{O}$ of water and temperature at which the reaction occurs (Lecuyer et al. 2010). Therefore, in living organisms it is expected that biomineralized materials are formed in equilibrium with body water. Previous studies with mammals confirmed that enamel $\delta^{18}\text{O}$ values reflect $\delta^{18}\text{O}$ values of ingested water (Longinelli 1984, Luz and Kolodny 1985, Iacumin et al. 1996, Podlesak et al. 2008); since mammals have a constant body temperature, the $\delta^{18}\text{O}_{\text{CO}_3}$ and $\delta^{18}\text{O}_{\text{PO}_4}$ values of bioapatite have a linear relationship with only slight variations in the reported equations and error (Bryant et al. 1996, Iacumin et al. 1996, Zazzo et al. 2004, Martin et al. 2008, Pellegrini et al. 2011, Chenery et al. 2012, Göhring et al. 2019).

In ectotherms, the oxygen isotope composition of bioapatite reflects both body water $\delta^{18}\text{O}$ values and the temperature at time of mineralization. Empirical relationships for environmental water $\delta^{18}\text{O}$ values, temperature, and $\delta^{18}\text{O}_{\text{PO}_4}$ values in biological apatite are established for fish (Longinelli and Nuti 1973, Kolodny et al. 1983). This relationship was applied to sharks by Vennemann et al. (2001), which resulted in expected temperature estimates of multiple species and their habitats. The equation was later revised with a study of captive fish (Pucéat et al. 2010). If both phosphate and carbonate oxygen isotope composition are forming in equilibrium with body water, similar to mammals, $\delta^{18}\text{O}_{\text{CO}_3}$ and $\delta^{18}\text{O}_{\text{PO}_4}$ values would have a strong linear relationship. However, our values of $\delta^{18}\text{O}_{\text{CO}_3}$ and $\delta^{18}\text{O}_{\text{PO}_4}$ have low correlation ($r = 0.44$, $p = 1.09 \times 10^{-6}$). This result is consistent with the larger variation in $\delta^{18}\text{O}_{\text{CO}_3}$ compared to $\delta^{18}\text{O}_{\text{PO}_4}$ values reported in Vennemann et al. (2001). With multiple studies showing a strong relationship between source water, temperature, and $\delta^{18}\text{O}_{\text{PO}_4}$ in fish, it is most likely that the variation we see in sharks is caused by an additional factor effecting $\delta^{18}\text{O}_{\text{CO}_3}$ values. A possible explanation for this lack of strong pattern is the incorporation of oxygen from DIC into the carbonate ion, as DIC has multiple ions with associated oxygen atoms (CO_2 , CO_3^{2-} , HCO_3^-).

4.1.2 Taxonomic patterns

Despite having low correlation across the sampled population, we found patterns in $\delta^{18}\text{O}_{\text{CO}_3}$ and $\delta^{18}\text{O}_{\text{PO}_4}$ values when examined by taxonomic family.

Carcharhinid sharks (*Carcharhinus brevipinna* n=1, *Carcharhinus leucas* n=19, *Carcharhinus limbatus* n=5, *Carcharhinus obscurus* n=5, *Carcharhinus plumbeus* n=15, *Galeocerdo cuvier* n=9) have a strong and significant correlation ($r = 0.70$, $p = 7.49 \times 10^{-9}$). In contrast, lamnid sharks (*Lamna ditropis* n=3, *Carcharodon carcharias* n=6) do not correlate ($r = -0.06$, $p = 0.88$) and instead group together with elevated $\delta^{18}\text{O}_{\text{CO}_3}$ values (Figure 2), likely due to their mesothermy, a form of thermoregulation that allows retention of some metabolic heat to elevate body temperature above their environment (Goldman 1997).

The Odontaspidid sharks (*Carcharias taurus* n=54, *Odontaspis ferox* n=3) also show an interesting pattern, with differentiation by species and habitat. In *C. taurus*, wild-caught and aquarium-kept individuals differentiate in $\delta^{18}\text{O}_{\text{PO}_4}$ values, as expected given stable water temperatures in captivity, but not in $\delta^{18}\text{O}_{\text{CO}_3}$ values (Figure 2, pink open circles). This pattern could be due to water treatment or additives at the aquarium that affect DIC isotope composition or due to the migratory pattern of wild *C. taurus*. Individuals sampled are part of a population in Delaware Bay that spends time in the low salinity waters of the bay and migrates along the coastal shelf (Kneebone et al. 2012, 2014, Teter et al. 2015). The *O. ferox* individuals have a similar range in $\delta^{18}\text{O}_{\text{PO}_4}$ values as the wild *C. taurus*, but differentiate in $\delta^{18}\text{O}_{\text{CO}_3}$ values, possibly due to their habitat preference for deeper water (Compagno 2001).

4.1.3 Oxygen offset as a metric for diagenesis

The carbonate-phosphate oxygen isotope spacing ($\delta^{18}\text{O}_{\text{CO}_3} - \delta^{18}\text{O}_{\text{PO}_4}$) has been proposed as diagnostic tool for diagenesis in fossils (e.g., Kohn and Cerling 2002). Previous studies on mammalian teeth suggest an expected offset of $\sim 9\text{‰}$ in unaltered samples and deviation from this range is interpreted as alteration (Bryant et al. 1996, Iacumin et al. 1996, Martin et al. 2008). Modern mammal studies generally report standard deviations of $< 1\text{‰}$. Despite close correlation between the two variables in mammals, a few studies still caution against reliance on this metric. For example, one study found an average spacing of $8.4 \pm 0.7\text{‰}$, but a large intra-tooth variation of $\sim 2\text{‰}$ (Martin et al. 2008). A literature review of mammalian oxygen isotope spacing concluded that despite strong correlation, the amount of variability in spacing means this measurement should not be used as a diagnostic tool for diagenesis until the water source of biapatite mineralization is better understood (Pellegrini et al. 2011). More recent studies suggest that this variability in oxygen isotope spacing may be related to species or diet-specific differences (Göhring et al. 2019) or impacted by seasonality (Fraser et al. 2021). Enameloid in bony fish has a reported offset of 8.1-11.0‰ in modern specimens and 6.8-11.7‰ in Holocene specimens (Sisma-Ventura et al. 2019). Similarly, we found this offset has a much larger range in modern sharks (Vennemann et al. 2001 range: 6.0-11.8‰ with an average of $9.1 \pm 1.5\text{‰}$; our data range: 0.3-7.5‰). Given the lack of correlation between $\delta^{18}\text{O}$ values from

carbonate and phosphate in our dataset as well as the larger variation in offset for modern sharks, this metric is not diagnostic of diagenesis in shark teeth.

4.2 Deconvolving carbon isotopes in shark teeth

4.2.1 Applications of stable isotope analysis in shark teeth

Stable isotope analysis is one of the primary techniques used to study modern shark ecology (Shiffman et al. 2020). Most of these studies analyze soft tissues for organic carbon and nitrogen to determine diet contribution, trophic level, and ontogenetic changes. Captive feeding studies have investigated tissue-specific incorporation rates and discrimination factors in sand tiger sharks (*C. taurus*), lemon sharks (*Negaprion brevirostris*), sandbar sharks (*Carcharhinus plumbeus*), leopard sharks (*Triakis semifasciata*), and the large-spotted dogfish (*Scyliorhinus stellaris*) (Hussey et al. 2010, Logan and Lutcavage 2010, Kim et al. 2012b, 2012a, Caut et al. 2013). Many studies use soft tissues (i.e., muscle) to answer modern ecological questions (Bird et al. 2018 and references within) by applying the previously mentioned tissue-specific incorporation rates and discrimination factors. However, there are relatively few modern studies that focus on materials that can be found in the fossil record (teeth/vertebrae) (Kim et al. 2012c, Carlisle et al. 2014).

Collagen extracted from mineralized tissues (teeth/vertebrae) has been used as an ecological proxy that records seasonal (Polo-Silva et al. 2012, Shipley et al. 2021) and annual variability (Estrada et al. 2006, Kerr et al. 2006, Werry et al. 2011, Kim et al. 2012c, Carlisle et al. 2014, Christiansen et al. 2014, Montaña et al. 2019, Raoult et al. 2019). In addition, there are discrimination factors estimated for collagen extracted from shark teeth (Zeichner et al. 2017) and vertebrae (Kim et al. 2012c). However, the inorganic carbon isotope values from these materials are rarely used or reported in the literature due to their abnormal values, which are often positive and lack an interpretative framework. Besides this study, there is only one other published dataset of inorganic carbon isotope values for modern sharks (Vennemann et al. 2001). There are a few paleontological studies reporting $\delta^{13}\text{C}_{\text{CO}_3}$ values for fossil shark teeth, however these values were not used to make paleoecological interpretations. Instead they are used to identify carbon excursions in stratigraphy and as a check for diagenesis (Ounis et al. 2008, Van Baal et al. 2013, Kocsis et al. 2014), or are reported alongside $\delta^{18}\text{O}_{\text{CO}_3}$ (Kolodny and Luz 1992, Aguilera et al. 2017).

Mammals are the most thoroughly studied taxa for SIA since they can be kept in captivity for controlled feeding studies and substrates for isotopic analysis are easily collected (i.e., breath, urine, feces, hair, etc.). The $\delta^{13}\text{C}$ values in organics and carbonate within mammalian teeth reflect diet. Previous studies with captive mammals investigated source, fractionation, and incorporation rates of ^{13}C in both soft (Tieszen et al. 1983, Hobson et al. 1996, Sponheimer et al. 2003) and hard (i.e., inorganic enamel and bone) tissues (Cerling and Harris

1999, Passey et al. 2005). These results demonstrated that carbon isotope compositions tracked diet and energy flow from the base of the food web. Further, the bulk of paleoecology studies using stable isotopes focus on terrestrial mammals and analyzed fossil teeth for $\delta^{13}\text{C}_{\text{CO}_3}$ values. These studies investigated the initiation and prevalence of different photosynthetic pathways (C3 vs. C4) of plants in the ecosystem (Farquhar et al. 1989), which can provide insight into environmental conditions such as temperature and aridity (Kohn 2010). The dominance of C3 vs. C4 plants is not relevant for ancient marine ecosystems, but if we can better understand the relationship between dietary carbon and $\delta^{13}\text{C}_{\text{CO}_3}$ values in shark enameloid we could address questions about nearshore vs. offshore environments, nutrient-rich upwelling regions, and productivity regimes in modern sharks and the fossil record. This is especially important in fossils, where dietary carbon is impossible to sample directly due to degradation.

4.2.2 Complications in using $\delta^{13}\text{C}_{\text{CO}_3}$ in sharks

Marine and aquatic organisms have a more complicated relationship with carbon isotope composition in biominerals due to the possible inclusion of dissolved inorganic carbon (DIC) during mineralization. There is low correspondence between $\delta^{13}\text{C}_{\text{CO}_3}$ and $\delta^{13}\text{C}_{\text{org}}$ values (Figure 3), which suggests that $\delta^{13}\text{C}_{\text{CO}_3}$ does not represent diet in sharks. There are other marine organisms with evidence that $\delta^{13}\text{C}_{\text{CO}_3}$ values record more than diet alone. For example, $\delta^{13}\text{C}_{\text{CO}_3}$ values of corals form in equilibrium with environmental water and vary with DIC and photosynthesis (McConnaughey et al. 1997). In fish otoliths, $\delta^{13}\text{C}_{\text{CO}_3}$ values are suggested to be a combined signal of diet, DIC, and metabolism that is best represented with a two-component mixing model (Chung et al. 2019).

This study includes individuals from a captive feeding study (Kim et al. 2012b), which supports the explanation that $\delta^{13}\text{C}_{\text{CO}_3}$ values do not solely represent diet in sharks. The leopard sharks (Family – Triakidae) were kept in similar water conditions but fed two isotopically distinct diets (i.e., squid $\delta^{13}\text{C} = -18.5 \pm 0.5\text{‰}$ and tilapia $\delta^{13}\text{C} = -23.2 \pm 0.9\text{‰}$). Although the sharks fed tilapia had distinct $\delta^{13}\text{C}_{\text{org}}$ values, their $\delta^{13}\text{C}_{\text{CO}_3}$ values were similar to our full dataset of wild sharks and squid-fed leopard sharks. Having isotopically distinct diets yet similar $\delta^{13}\text{C}_{\text{CO}_3}$ values indicates the carbonate substrate is not tracking diet with high fidelity. However, all the captive leopard sharks shared the same water conditions, which suggests the incorporation of an environmental factor, such as DIC, similar to fish otoliths.

We also observed that this phenomenon was limited to oxygen isotope composition of carbonate, but not phosphate. There was a strong positive relationship of ϵ with $\delta^{18}\text{O}_{\text{CO}_3}$ values ($r^2 = 0.62$, $p < 2.2 \times 10^{-16}$), but not with $\delta^{18}\text{O}_{\text{PO}_4}$ values ($r^2 = 0.04$, $p = 0.03$), which suggests that the unusual carbon isotope values in shark enameloid are likely related to carbonate ion (CO_3^{2-})

substitutions rather than isolated to $\delta^{13}\text{C}_{\text{CO}_3}$ values. If during the enameloid maturation process DIC is incorporated or exchanged in the mineral matrix, then it would affect both $\delta^{13}\text{C}_{\text{CO}_3}$ and $\delta^{18}\text{O}_{\text{CO}_3}$ values. We develop a model based on modern teeth to estimate the $\delta^{13}\text{C}_{\text{org}}$ values of shark teeth from carbonate isotope composition, which has application for paleoecological studies of carbon cycling, diet, and food web dynamics of ancient marine ecosystems.

4.3 Estimated fossil organic carbon values

The possibility to estimate organic carbon isotope values from shark teeth reveals potential ecological and environmental information about ancient marine ecosystems. Organic carbon isotope values likely vary through geologic time depending on the carbon cycling processes, but studies must rely on inorganic carbon rock record since organic carbon has long been lost to diagenesis. We estimated $\delta^{13}\text{C}_{\text{org}}$ values for fossil shark teeth using a linear model based on modern shark teeth (Figure 4). In general, the average $\delta^{13}\text{C}_{\text{org}}^*$ value decreases over time so that Pliocene sharks are most similar to modern sharks, a trend also documented in the benthic foraminifera record (Zachos et al. 2001). The anomaly to this pattern is during the Eocene, which has the highest variability with mean $\delta^{13}\text{C}_{\text{org}}^*$ values = $-3.3 \pm 5.9\%$. There are two possible explanations for this high carbon isotope variability during the Eocene. First, many of our samples are from the Eureka Sound Formation on Banks Island in the Arctic where $\delta^{18}\text{O}$ values from shark enameloid indicate brackish water (Kim et al. 2014), which would affect DIC (Bakker et al. 1999, Gillikin et al. 2006). Second, the Eocene is characterized as greenhouse climate conditions with high mean global temperatures, high concentrations of atmospheric CO_2 , and punctuated climate events characterized by negative carbon isotope excursions (Zachos et al. 2008). These climate events include longer events such as the Early Eocene Climatic Optimum (EECO) and more rapid events known as hyperthermals (such as the Paleocene-Eocene Thermal Maximum (PETM), the best studied and most extreme Eocene hyperthermal). The possibility to estimate $\delta^{13}\text{C}_{\text{org}}^*$ values based on carbonate SIA in shark teeth presents opportunities to extend SIA applications beyond environmental reconstruction and to ecological questions.

5. Conclusions

In conclusion, we compiled and analyzed the largest dataset to date of stable isotope values comparing multiple substrates in modern and fossil shark teeth. This study provides a foundation for the use of shark teeth beyond environmental reconstructions to dig deeper into shark paleoecology. Due to poor correlation between $\delta^{18}\text{O}_{\text{CO}_3}$ and $\delta^{18}\text{O}_{\text{PO}_4}$ values, we suggest only using $\delta^{18}\text{O}_{\text{PO}_4}$ values from shark enameloid as a proxy for temperature or water $\delta^{18}\text{O}$ values. Additionally, the carbonate-phosphate oxygen isotope spacing ($\delta^{18}\text{O}_{\text{CO}_3} -$

$\delta^{18}\text{O}_{\text{PO}_4}$) should not be used as a diagnostic tool for diagenetic alteration in shark teeth because there is a significant amount of variation among modern teeth, which have no possibility for diagenetic alteration. In sharks, $\delta^{13}\text{C}_{\text{CO}_3}$ values do not correlate with $\delta^{13}\text{C}_{\text{org}}$ values and therefore does not trace diet. Instead, $\delta^{13}\text{C}_{\text{CO}_3}$ values reflect a combined diet and DIC signal, similar to fish otoliths. This hypothesis is supported by the relationship between carbon fractionation ϵ and $\delta^{18}\text{O}_{\text{CO}_3}$ values. The model from this relationship was tested on a fossil dataset of 54 samples that included ones from the Cretaceous, Eocene, Miocene, and Pliocene. It allows estimation of $\delta^{13}\text{C}_{\text{org}}^*$ values from fossil tooth enameloid, which indicate ^{13}C enrichment through time. This trend provides a basis to investigate carbon cycling and food web dynamics in ancient marine environments using fossil shark teeth.

Works Cited

- Aguilera, O., Z. Luz, J. D. Carrillo-Briceño, L. Kocsis, T. W. Vennemann, P. M. De Toledo, A. Nogueira, K. B. Amorim, H. Moraes-Santos, M. R. Polck, M. de L. Ruivo, A. P. Linhares, and C. Monteiro-Neto. 2017. Neogene sharks and rays from the Brazilian 'Blue Amazon.' *PLoS ONE* 12:1–34.
- Van Baal, R. R., R. Janssen, H. J. L. van der Lubbe, A. S. Schulp, J. W. M. Jagt, and H. B. Vonhof. 2013. Oxygen and carbon stable isotope records of marine vertebrates from the type Maastrichtian, The Netherlands and northeast Belgium (Late Cretaceous). *Palaeogeography, Palaeoclimatology, Palaeoecology* 392:71–78.
- Bakker, D. C. E., H. J. W. De Baar, and E. De Jong. 1999. The dependence on temperature and salinity of dissolved inorganic carbon in East Atlantic surface waters. *Marine Chemistry* 65:263–280.
- Berkovitz, B. K. B., and R. P. Shellis. 2017a. Tooth Replacement and Ontogeny of the Dentition. Pages 255–289 *The Teeth of Non-Mammalian Vertebrates*.
- Berkovitz, B., and P. Shellis. 2017b. Enameloid and Enamel. Pages 311–330 *The Teeth of Non-Mammalian Vertebrates*.
- Bird, C. S., A. Veríssimo, S. Magozzi, K. G. Abrantes, A. Aguilar, H. Al-Reasi, A. Barnett, D. M. Bethea, G. Biais, A. Borrell, M. Bouchoucha, M. Boyle, E. J. Brooks, J. Brunnschweiler, P. Bustamante, A. Carlisle, D. Catarino, S. Caut, Y. Cherel, T. Chouvelon, D. Churchill, J. Ciancio, J. Claes, A. Colaço, D. L. Courtney, P. Cresson, R. Daly, L. De Necker, T. Endo, I. Figueiredo, A. J. Frisch, J. H. Hansen, M. Heithaus, N. E. Hussey, J. Iitembu, F. Juanes, M. J. Kinney, J. J. Kiszka, S. A. Klarian, D. Kopp, R. Leaf, Y. Li, A. Lorrain, D. J. Madigan, A. Maljković, L. Malpica-Cruz, P. Matich, M. G. Meekan, F. Ménard, G. M. Menezes, S. E. M. Munroe, M. C. Newman, Y. P. Papastamatiou, H. Pethybridge, J. D. Plumlee, C. Polo-Silva, K. Quaeck-Davies, V. Raoult, J. Reum, Y. E. Torres-Rojas, D. S. Shiffman, O. N. Shipley, C. W. Speed, M. D. Staudinger, A. K. Teffer, A. Tilley, M. Valls, J. J. Vaudo, T. C. Wai, R. J. D. Wells, A. S. J. Wyatt, A. Yool, and C. N. Trueman. 2018. A global perspective on the trophic geography of sharks. *Nature Ecology and Evolution* 2:299–305.
- Bryant, J. D., P. L. Koch, P. N. Froelich, W. J. Showers, and B. J. Genna. 1996. Oxygen isotope partitioning between phosphate and carbonate in mammalian apatite. *Geochimica et Cosmochimica Acta* 60:5145–5148.
- Carlisle, A. B., K. J. Goldman, S. Y. Litvin, D. J. Madigan, J. S. Bigman, A. M. Swithenbank, T. C. J. Kline, and B. A. Block. 2014. Stable isotope analysis of vertebrae reveals ontogenetic changes in habitat in an endothermic pelagic shark. *Proceedings of the Royal Society B* 282.

- Casey, M. M., and D. M. Post. 2011. The problem of isotopic baseline: Reconstructing the diet and trophic position of fossil animals. *Earth-Science Reviews* 106:131–148.
- Caut, S., M. J. Jowers, L. Michel, G. Lepoint, and A. T. Fisk. 2013. Diet-and tissue-specific incorporation of isotopes in the shark *Scyliorhinus stellaris*, a North Sea mesopredator. *Marine Ecology Progress Series* 492:185–198.
- Cerling, T. E., and J. M. Harris. 1999. Carbon isotope fractionation for ecological mammals and implications for ecological and paleoecological studies. *Oecologia* 120:347–363.
- Chenery, C. A., V. Pashley, A. L. Lamb, H. J. Sloane, and J. A. Evans. 2012. The oxygen isotope relationship between the phosphate and structural carbonate fractions of human bioapatite. *Rapid Communications in Mass Spectrometry*:309–319.
- Christiansen, H. M., N. E. Hussey, S. P. Wintner, G. Cliff, S. F. J. Dudley, and A. T. Fisk. 2014. Effect of sample preparation techniques for carbon and nitrogen stable isotope analysis of hydroxyapatite structures in the form of elasmobranch vertebral centra. *Rapid Communications in Mass Spectrometry* 28:448–456.
- Chung, M. T., C. N. Trueman, J. A. Godiksen, and P. Grønkjær. 2019. Otolith $\delta^{13}\text{C}$ values as a metabolic proxy: Approaches and mechanical underpinnings. *Marine and Freshwater Research* 70:1747–1756.
- Codron, D., M. Clauss, J. Codron, and T. Tütken. 2018. Within trophic level shifts in collagen–carbonate stable carbon isotope spacing are propagated by diet and digestive physiology in large mammal herbivores. *Ecology and Evolution* 8:3983–3995.
- Compagno, L. J. V. 2001. Order LAMNIFORMES - Mackerel sharks. Pages 51–67 *Sharks of the World: An Annotated and Illustrated Catalogue of Shark Species Known to Date*.
- DeNiro, M. J., and S. Epstein. 1978. Influence of diet on the distribution of carbon isotopes in animals*. *Geochimica et Cosmochimica Acta* 42:495–506.
- Enax, J., A. M. Janus, D. Raabe, M. Epple, and H. O. Fabritius. 2014. Ultrastructural organization and micromechanical properties of shark tooth enameloid. Pages 3959–3968 *Acta Biomaterialia*. Elsevier Ltd.
- Enax, J., O. Prymak, D. Raabe, and M. Epple. 2012. Structure, composition, and mechanical properties of shark teeth. *Journal of Structural Biology* 178:290–299.

- Estrada, J. A., A. N. Rice, L. J. Natanson, and G. B. Skomal. 2006. USE OF ISOTOPIC ANALYSIS OF VERTEBRAE IN RECONSTRUCTING ONTOGENETIC FEEDING ECOLOGY IN WHITE SHARKS. *Ecology* 87:829–834.
- Farquhar, G. D., J. R. Ehleringer, and K. T. Hubick. 1989. Carbon Isotope Discrimination and Photosynthesis. *Annual Review of Plant Physiology and Plant Molecular Biology* 40:503–537.
- Fischer, J., S. Voigt, M. Franz, J. W. Schneider, M. M. Joachimski, M. Tichomirowa, J. Götze, and H. Furrer. 2012. Palaeoenvironments of the late Triassic Rhaetian Sea: Implications from oxygen and strontium isotopes of hybodont shark teeth. *Palaeogeography, Palaeoclimatology, Palaeoecology* 353–355:60–72.
- Gillikin, D. P., A. Lorrain, S. Bouillon, P. Willenz, and F. Dehairs. 2006. Stable carbon isotopic composition of *Mytilus edulis* shells: relation to metabolism, salinity, $\delta^{13}\text{C}_{\text{DIC}}$ and phytoplankton. *Organic Geochemistry* 37:1371–1382.
- Göhring, A., C. von Carnap-Bornheim, V. Hilberg, C. Mayr, and G. Grupe. 2019. Diet and species-specific oxygen isotope relationship and isotope spacing between structural carbonate and phosphate in archaeological mammalian bones. *Archaeological and Anthropological Sciences* 11:2467–2487.
- Goldman, K. J. 1997. Regulation of body temperature in the white shark , *Carcharodon carcharias*. *Journal of Comparative Physiology B* 167:423–429.
- Hättig, K., K. Stevens, D. Thies, G. Schweigert, J. Mutterlose, I. Geologie, and L. Hannover. 2019. Evaluation of shark tooth diagenesis-screening methods and the application of their stable oxygen isotope data for palaeoenvironmental reconstructions. *Journal of the Geological Society* 176:482–491.
- Hobson, K. A., D. M. Schell, D. Renouf, and E. Noseworthy. 1996. Stable carbon and nitrogen isotopic fractionation between diet and tissues of captive seals : implications for dietary reconstructions involving marine mammals. *Canadian Journal of Fisheries and Aquatic Sciences* 53:528–533.
- Hussey, N. E., J. Brush, I. D. McCarthy, and A. T. Fisk. 2010. $\delta^{15}\text{N}$ and $\delta^{13}\text{C}$ diet-tissue discrimination factors for large sharks under semi-controlled conditions. *Comparative Biochemistry and Physiology - A Molecular and Integrative Physiology* 155:445–453.
- Iacumin, P., H. Bocherens, A. Mariotti, and A. Longinelli. 1996. Oxygen isotope analyses of co-existing carbonate and phosphate in biogenic apatite: a way to monitor diagenetic alteration of bone phosphate? *Earth and Planetary Science Letters* 142:1–6.

- Kast, E. R., M. L. Griffiths, S. L. Kim, Z. C. Rao, K. Shimada, M. A. Becker, H. M. Maisch, R. A. Eagle, C. A. Clarke, A. N. Neumann, M. E. Karnes, T. Ludecke, J. N. Leichliter, A. Martinez-Garcia, A. A. Akhtar, X. T. Wang, G. H. Haug, D. M. Sigman. 2022. Science Advances (Accpeted).
- Kerr, L. A., A. H. Andrews, G. M. Cailliet, T. A. Brown, and K. H. Coale. 2006. Investigations of D14C, d13C, and d15N in vertebrae of white shark (*Carcharodon carcharias*) from the eastern North Pacific Ocean. *Environmental Biology of Fishes* 77:337–353.
- Kim, S. L., D. R. Casper, F. Galván-Magaña, R. Ochoa-Díaz, S. B. Hernández-Aguilar, and P. L. Koch. 2012a. Carbon and nitrogen discrimination factors for elasmobranch soft tissues based on a long-term controlled feeding study. *Environmental Biology of Fishes* 95:37–52.
- Kim, S. L., J. J. Eberle, D. M. Bell, D. A. Fox, and A. Padilla. 2014. Evidence from shark teeth for a brackish Arctic Ocean in the Eocene greenhouse Evidence from shark teeth for a brackish Arctic Ocean in the Eocene. *Geology*.
- Kim, S. L., C. M. Del Rio, D. Casper, and P. L. Koch. 2012b. Isotopic incorporation rates for shark tissues from a long-Term captive feeding study. *Journal of Experimental Biology* 215:2495–2500.
- Kim, S. L., M. T. Tinker, J. A. Estes, and P. L. Koch. 2012c. Ontogenetic and Among-Individual Variation in Foraging Strategies of Northeast Pacific White Sharks Based on Stable Isotope Analysis. *PLoS ONE* 7.
- Kim, S. L., S. S. Zeichner, A. S. Colman, H. D. Scher, J. Kriwet, T. Mörs, and M. Huber. 2020. Probing the Ecology and Climate of the Eocene Southern Ocean With Sand Tiger Sharks *Striatolamia macrota*. *Paleoceanography and Paleoclimatology* 35:1–21.
- Kneebone, J., J. Chisholm, and G. Skomal. 2014. Movement patterns of juvenile sand tigers (*Carcharias taurus*) along the east coast of the USA. *Marine Biology* 161:1149–1163.
- Kneebone, J., J. Chisholm, and G. B. Skomal. 2012. Seasonal residency, habitat use, and site fidelity of juvenile sand tiger sharks *Carcharias taurus* in a Massachusetts estuary. *Marine Ecology Progress Series* 471:165–181.
- Kocsis, L., E. Gheerbrant, M. Mouflih, H. Cappetta, J. Yans, and M. Amaghazaz. 2014. Comprehensive stable isotope investigation of marine biogenic apatite from the late Cretaceous-early Eocene phosphate series of Morocco. *Palaeogeography, Palaeoclimatology, Palaeoecology* 394:74–88.
- Kohn, M. J. 2010. Carbon isotope compositions of terrestrial C3 plants as indicators of (paleo) ecology and (paleo) climate. *Proceedings of the National Academy of Sciences* 107:19691–19695.

- Kohn, M. J., and T. E. Cerling. 2002. Stable isotope compositions of biological apatite. *Phosphates: Geochemical, Geobiological and Materials Importance* 48:455–488.
- Kolodny, Y., and B. Luz. 1992. The isotopic record of oxygen in phosphates of fossil fish - Devonian to Recent. *The Paleontological Society Special Publications*:105–119.
- Kolodny, Y., B. Luz, and O. Navon. 1983. Oxygen isotope variations in phosphate of biogenic apatites, I. Fish bone apatite-rechecking the rules of the game. *Earth and Planetary Science Letters* 64:398–404.
- Lecuyer, C., V. Balter, F. Martineau, F. Fourel, A. Bernard, R. Amiot, V. Gardien, O. Otero, S. Legendre, G. Panczer, L. Simon, and R. Martini. 2010. Oxygen isotope fractionation between apatite-bound carbonate and water determined from controlled experiments with synthetic apatites precipitated at 10 – 37 ° C. *Geochimica et Cosmochimica Acta* 74:2072–2081.
- Lecuyer, C., S. Picard, J.-P. Garcia, S. M. F. Sheppard, P. Grandjean, and G. Dromart. 2003. Thermal evolution of Tethyan surface waters during the Middle-Late Jurassic Evidence. *Paleoceanography* 18.
- Logan, J. M., and M. E. Lutcavage. 2010. Stable isotope dynamics in elasmobranch fishes. *Hydrobiologia* 644:231–244.
- Longinelli, A. 1984. Oxygen isotopes in mammal bone phosphate : A new tool for paleohydrological and paleoclimatological research ? *Geochimica et Cosmochimica Acta* 48:385–390.
- Longinelli, A., and S. Nuti. 1973. OXYGEN ISOTOPE MEASUREMENTS OF PHOSPHATE FROM FISH TEETH AND BONES. *Earth and Planetary Science Letters* 20:337–340.
- Luz, B., and Y. Kolodny. 1985. Oxygen isotope variations in phosphate of biogenic apatites , IV . Mammal teeth and bones. *Earth and Planetary Science Letters* 75:29–36.
- Martin, C., I. Bentaleb, R. Kaandorp, P. Iacumin, and K. Chatri. 2008. Intra-tooth study of modern rhinoceros enamel $\delta^{18}\text{O}$: Is the difference between phosphate and carbonate $\delta^{18}\text{O}$ a sound diagenetic test ? *Palaeogeography, Palaeoclimatology, Palaeoecology* 266:183–189.
- McConnaughey, T. A., J. Burdett, J. F. Whelan, and C. K. Paull. 1997. Carbon isotopes in biological carbonates: Respiration and photosynthesis. *Geochimica et Cosmochimica Acta* 61:611–622.
- McCormack J., M. L. Griffiths, S. L. Kim, K. Shimada, M. Karnes, H. Maisch IV, S. Pederzani, N. Bourgon, K. Jouen, M. A. Becker, N. Jons, G. Sisma-Ventura, N. Straube, J. Pollerspöck, J. J. Hublin, R. A. Eagle, T. Tutken. 2022. *Nature Communications*. (Accepted).

- Miake, Y., T. Aoba, E. C. Moreno, S. Shimoda, K. Probst, and S. Suga. 1991. Ultrastructural studies on crystal growth of enameloid minerals in elasmobranch and teleost fish. *Calcified Tissue International* 48:204–217.
- Mine, A. H., A. Waldeck, G. Olack, M. E. Hoerner, S. Alex, and A. S. Colman. 2017. Microprecipitation and $\delta^{18}\text{O}$ analysis of phosphate for paleoclimate and biogeochemistry research. *Chemical Geology* 460:1–14.
- Moeller, I. J., B. Melsen, S. J. Jensen, and E. Kirkegaard. 1975. A histological, chemical and X-ray diffraction study on contemporary (*Carcharias glaucus*) and fossilized (*Macrota odontaspis*) shark teeth. *Archives of Oral Biology* 20.
- Montaño, C. E., F. Galván, M. Alberto, and S. González. 2019. Dietary ontogeny of the blue shark, *Prionace glauca*, based on the analysis of $\delta^{13}\text{C}$ and $\delta^{15}\text{N}$ in vertebrae. *Marine Biology* 166:1–13.
- Unis, A., L. Kocsis, F. Chaabani, and H. R. Pfeifer. 2008. Rare earth elements and stable isotope geochemistry ($\delta^{13}\text{C}$ and $\delta^{18}\text{O}$) of phosphorite deposits in the Gafsa Basin, Tunisia. *Palaeogeography, Palaeoclimatology, Palaeoecology* 268:1–18.
- Passey, B. H., T. F. Robinson, L. K. Ayliffe, T. E. Cerling, M. Sponheimer, M. D. Dearing, B. L. Roeder, and J. R. Ehleringer. 2005. Carbon isotope fractionation between diet, breath CO_2 , and bioapatite in different mammals. *Journal of Archaeological Science* 32:1459–1470.
- Pellegrini, M., J. A. Lee-thorp, and R. E. Donahue. 2011. Exploring the variation of the $\delta^{18}\text{O}_p$ and $\delta^{18}\text{O}_c$ relationship in enamel increments. *Palaeogeography, Palaeoclimatology, Palaeoecology* 310:71–83.
- Podlesak, D. W., A. Torregrossa, J. R. Ehleringer, M. D. Dearing, B. H. Passey, and T. E. Cerling. 2008. Turnover of oxygen and hydrogen isotopes in the body water, CO_2 , hair, and enamel of a small mammal. *Geochimica et Cosmochimica Acta* 72:19–35.
- Polo-Silva, C. J., F. Galván-Magaña, and A. Delgado-Huertas. 2012. Trophic inferences of blue shark (*Prionace glauca*) in the Mexican Pacific from stable isotope analysis in teeth. *Rapid Communications in Mass Spectrometry* 26:1631–1638.
- Pucéat, E., M. M. Joachimski, A. Bouilloux, F. Monna, A. Bonin, S. Motreuil, P. Morinière, S. Hénard, J. Mourin, G. Dera, and D. Quesne. 2010. Revised phosphate-water fractionation equation reassessing paleotemperatures derived from biogenic apatite. *Earth and Planetary Science Letters* 298:135–142.
- Raoult, V., T. F. Gaston, M. K. Broadhurst, V. M. Peddemors, and J. E. Williamson. 2019. Resource use of great hammerhead sharks (*Sphyrna mokarran*) off eastern Australia. *Journal of Fish Biology* 95:1430–1440.

- Shiffman, D. S., M. J. Ajemian, J. C. Carrier, T. S. Daly-Engel, M. M. Davis, N. K. Dulvy, R. D. Grubbs, N. A. Hinojosa, J. Imhoff, M. A. Kolmann, C. S. Nash, E. W. M. Paig-Tran, E. E. Peele, R. A. Skubel, B. M. Wetherbee, L. B. Whitenack, and J. T. Wyffels. 2020. Trends in Chondrichthyan Research: An Analysis of Three Decades of Conference Abstracts. *Copeia* 108:122–131.
- Shipley, O. N., G. A. Henkes, J. Gelsleichter, C. R. Morgan, E. V. Schneider, B. S. Talwar, and M. G. Frisk. 2021. Shark tooth collagen stable isotopes ($\delta^{15}\text{N}$ and $\delta^{13}\text{C}$) as ecological proxies. *Journal of Animal Ecology* 90:2188–2201.
- Sire, J. Y., T. Davit-Béal, S. Delgado, and X. Gu. 2007. The origin and evolution of enamel mineralization genes. *Cells Tissues Organs* 186:25–48.
- Sisma-Ventura, G., T. Tutken, S. T. M. Peters, O. M. Bialik, I. Zohar, and A. Pack. 2019. Past aquatic environments in the Levant inferred from stable isotope compositions of carbonate and phosphate in fish teeth. *PLoS ONE* 14:1–18.
- Sponheimer, M., T. Robinson, L. Ayliffe, B. Passey, B. Roeder, L. Shipley, E. Lopez, T. Cerling, D. Dearing, and J. Ehleringer. 2003. An experimental study of carbon-isotope fractionation between diet, hair, and feces of mammalian herbivores. *Canadian Journal of Zoology* 81:871–876.
- Teter, S. M., B. M. Wetherbee, D. A. Fox, C. H. Lam, D. A. Kiefer, and M. Shivji. 2015. Migratory patterns and habitat use of the sand tiger shark (*Carcharias taurus*) in the western North Atlantic. *Marine and Freshwater Research* 66:158–169.
- Tieszen, L. L., T. W. Boutton, K. G. Tesdahl, and N. A. Slade. 1983. Fractionation and turnover of stable carbon isotopes in animal tissues: Implications for $\delta^{13}\text{C}$ analysis of diet. *Oecologia* 57:32–37.
- Trayler, R. B., P. Valencia Landa, S. L. Kim. In prep. Evaluating the Efficacy of Bone Collagen Isolation Using Stable Isotope Analysis and Infrared Spectroscopy.
- Trueman, C. N. G., A. K. Behrensmeyer, N. Tuross, and S. Weiner. 2004. Mineralogical and compositional changes in bones exposed on soil surfaces in Amboseli National Park, Kenya: Diagenetic mechanisms and the role of sediment pore fluids. *Journal of Archaeological Science* 31:721–739.
- Tütken, T., M. Weber, I. Zohar, H. Helmy, N. Bourgon, O. Lernau, K. P. Jochum, and G. Sisma-Ventura. 2020. Strontium and Oxygen Isotope Analyses Reveal Late Cretaceous Shark Teeth in Iron Age Strata in the Southern Levant. *Frontiers in Ecology and Evolution* 8.

- Vennemann, T. W., and E. Hegner. 1998. Oxygen, strontium, and neodymium isotope composition of fossil shark teeth as a proxy for the palaeoceanography and palaeoclimatology of the Miocene northern Alpine Paratethys. *Palaeogeography, Palaeoclimatology, Palaeoecology* 142:107–121.
- Vennemann, T. W., E. Hegner, G. Cliff, and G. W. Benz. 2001. Isotopic composition of recent shark teeth as a proxy for environmental conditions. *Geochimica et Cosmochimica Acta* 65:1583–1599.
- Werry, J. M. A., S. Y. A. Lee, N. M. C. Otway, Y. D. Hu, and W. E. Sumpton. 2011. A multi-faceted approach for quantifying the estuarine] nearshore transition in the life cycle of the bull shark , *Carcharhinus leucas*. *Marine and Freshwater Research* 62:1421–1431.
- Zachos, J. C., G. R. Dickens, and R. E. Zeebe. 2008. An early Cenozoic perspective on greenhouse warming and carbon-cycle dynamics. *Nature* 451:279–283.
- Zacke, A., S. Voigt, M. M. Joachimski, A. S. Gale, D. J. Ward, and T. Tutken. 2009. Surface-water freshening and high-latitude river discharge in the Eocene. *Journal of the Geological Society* 166:969–980.
- Zazzo, A., C. Lecuyer, S. M. F. Sheppard, P. Grandjean, and A. Mariotti. 2004. Diagenesis and the reconstruction of paleoenvironments : A method to restore original d18 O values of carbonate and phosphate from fossil tooth enamel. *Geochimica et Cosmochimica Acta* 68:2245–2258.
- Zeichner, S. S., A. S. Colman, P. L. Koch, C. Polo-Silva, F. Galván-Magaña, and S. L. Kim. 2017. Discrimination factors and incorporation rates for organic matrix in shark teeth based on a captive feeding study. *Physiological and Biochemical Zoology* 90:257–272.